Virus recognition with terahertz radiation: drawbacks and potentialities

Journal of Physics: Photonics

OPEN ACCESS

RECEIVED
4 December 2020

REVISED
4 March 2021

ACCEPTED FOR PUBLICATION
29 April 2021

PUBLISHED
19 May 2021

TOPICAL REVIEW

Virus recognition with terahertz radiation: drawbacks and potentialities

Marta Di Fabrizio[1,*], **Stefano Lupi**[1,2] **and Annalisa D'Arco**[3,*]

[1] Physics Department, University of Rome 'La Sapienza', Piazzale Aldo Moro 5, 00185 Rome, Italy
[2] INFN-LNF Via E. Fermi 40, 00044 Frascati, Italy
[3] INFN—section of Rome 'La Sapienza', P.le Aldo Moro 2, 00185 Rome, Italy
[*] Authors to whom any correspondence should be addressed.

E-mail: martadifabrizio@gmail.com **and** annalisa.darco@roma1.infn.it

Keywords: THz radiation, THz spectroscopy, virus detection, THz virus sensing, metamaterials, nanomaterials

Abstract

Virus sensing is earning great interest for recognition of dangerous and widely spread diseases, such as influenza A (virus subtypes H1N1, H3N2 etc), severe acute respiratory syndrome, Middle East respiratory syndrome etc. Many molecular and biological techniques have been developed and adopted for virus detection purposes. These techniques show some drawbacks concerning long collection time and data analysis, sensitivity, safety, costs etc. Therefore, new sensing approaches have been proposed for overcoming these limitations. In this short-review, we explore the emerging and challenging terahertz radiation technology and its applications to virus high-sensitivity remote-sensing devices.

1. Introduction

A virus is a pathogenic agent that is able to replicate only inside host living cells, parasitizing the cellular biosynthetic system. Its diameter typically ranges between ∼20 and ∼300 nm [1–3]. When a host cell is infected, an avalanche effect arises because the infecting virus forces the replication of its genetic material. Virus infection can spread in many ways, for instance by coughing and sneezing [4, 5], by ingesting infected food and/or water [6, 7], by sexual contact [8–10], by punctures of blood-sucking insects [11] etc. Therefore, rapid and effective techniques for virus sensing and recognition are becoming of vital importance. A fast and accurate monitoring can help to prevent wide transmission, spreading of viral infection and to carry out timely therapeutic treatment, disease control and surveillance. Nowadays, this is a crucial point, especially during the Covid-19 pandemic situation that is affecting our lives. This emergency, in fact, has imposed a severe burden on society and has led to the urgent need of effective virus diagnostic methods. Actually, many molecular and biological techniques are conventionally used. They include reverse transcription polymerase chain reaction (RT-PCR) [6, 12], reverse transcription loop-mediated isothermal amplification (RT-LAMP) [13, 14] and CRISPR–Cas13-based SHERLOCK system [15, 16]. In addition to those techniques, microfluidic biosensors are also considered [17–20]. In box 1 we report a brief summary concerning the most conventional molecular virus-detection techniques.

Box 1: Molecular techniques for virus detection

Nucleic acid and protein based methods are the most common molecular techniques for virus recognition. Nucleic acid based methods investigate virus nucleotide sequences or genes in biological patient's samples (fluids, washes, aspirates etc) [21]. Protein based methods, instead, look at viral protein antigens and antibodies, created by the immune system, in response to a viral infection [22].

Nucleic acid testing. The RT-PCR combines two techniques: the RT and PCR [6, 12]. The RT allows to recognize the genetic information. A RNA single strand transcription is made and a complementary strand (cDNA) is synthetized. The classic PCR instead, amplifies specific regions of cDNA, making them detectable [21]. Branched-chain DNA (bDNA) assay [23, 24] detects and quantifies nucleic acid targets. The main difference with RT-PCR is the direct measurement of RNA or DNA molecules at physiological levels by amplifying signals, rather than by amplifying sequences. As a general observation, bDNA shows a lower sensitivity than the RT-PCR technique [25].

Protein testing. Protein testing exploits the type-specific antibody response produced in response to the viral infection, looking for antibodies in blood serum or plasma [21]. Among protein testing, serological tests have been largely used in many virus types detection, from herpes simplex virus [26], to varicella-zoster virus [27], zika virus (ZIKV) [28] and severe acute respiratory syndrome-CoV-2 [29–31]. The effective result of these tests hardly depends on the immune system response. Therefore, the antibodies quantity imposes a limit of detection during the measurement. enzyme-linked immunosorbent assay (ELISA) [32, 33] is a biochemical test for the detection of antibody-antigen binding reaction. The presence of the antigen can be detected, with the help of an antibody-enzyme complex and a chromogen. A chromogenic substrate, in fact, yields a visible color change or fluorescence when interacting with the enzyme.

However, the above mentioned assays are time-consuming, labor-intensive and no reagent-free [21, 25]. Therefore, a complementary, fast, sensitive and non invasive alternative is highly desirable. In the following sections, an overview concerning the most promising terahertz (THz) technology approaches virus monitoring and detection will be presented and discussed.

2. THz spectroscopy

In the last decades, technology has experienced a wide diffusion of customizable and flexible THz systems for spectroscopic and imaging applications [34–38]. These systems found challenging applications in many science fields, like biology and medicine [37, 39–41], gas sensing [42, 43], material science [44, 45], chemical analysis and identification [46, 47] etc. THz radiation is largely appealing for biomedical issues because its low photon energy (4 meV @ 1 THz [48]) and its high penetration in anhydrous targets enable nondestructive and non-ionizing sensing. This is in contrast with other optical techniques, including ultraviolet or x-rays, where the high energy photons (>>eV) can cause direct biological damage on the sample [48–50]. In addition, many rotational and vibrational energy levels are located within the THz spectral range [48, 51] providing chemical specificity to imaging experiments, which can be efficiently done in label-free and non-contact modes [34, 37, 52]. However, THz radiation suffers from poor spatial resolution due to its large wavelength ($\lambda = 300\ \mu$m @ 1 THz) [53]. Detecting tiny microorganisms such as bacteria and viruses is very challenging because their lateral dimensions are strongly sub-diffraction [25]. In addition, the extreme sensitivity of THz radiation to polar molecules, specifically water, limits THz waves penetrability from tens to hundred microns in hydrated samples, preventing wide technological spread in biological fields [35, 48, 51, 52]. Regardless of these constraints, several THz investigations have been performed on biological materials [39, 52, 54]. For instance, Lee *et al* [50] exploited THz spectroscopy for measuring THz absorbance of H9N2 virus sample, in the spectral range from 0.2 to 2 THz. As it can be seen in figure 1 the freeze-dried pellet virus sample absorption is practically identical to the substrate, showing no identifiable spectral features.

Authors assigned the case to superposition of many protein vibration modes and inhomogeneous broadening of absorption features [50]. This suggests that the weak THz detection sensitivity and low chemical specificity are the main obstacles for THz sensing applications in pathogenic monitoring.

Interestingly, Sun and coauthors [55] used their THz-time domain spectroscopy (THz-TDS) system in transmission mode to assess an indirect virus detection modality. They investigated the binding properties of H9 HA protein and its specific human monoclonal antibody F10. H9 HA protein is the main surface glycoprotein of the Avian influenza (AI) virus and F10 is its specific antibody. Sun and the authors

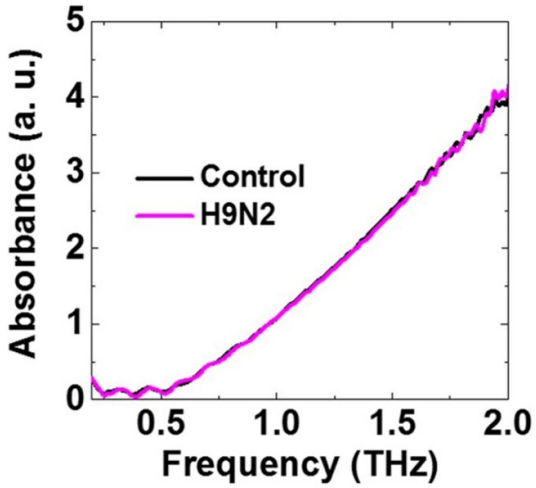

Figure 1. Absorbance vs frequency of H9N2 virus freeze-dried pellet (pink) and control (black) samples [50].

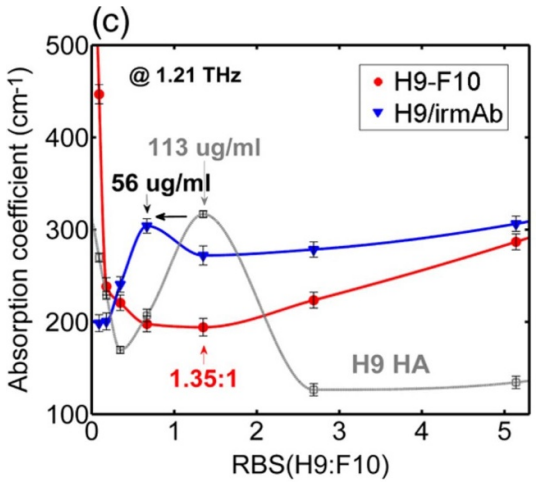

Figure 2. Absorption coefficient vs ratio of binding sites (RBS) for H9 HA-F10 (red) and H9 HA-irmAb (blue) samples, compared to H9 NA sample [55]. RBS takes into account H9 HA protein and antibody concentrations.

demonstrated that THz spectroscopy is sensitive to the antibody-antigen reaction, by looking at the changes in the hydration shell around H9 HA molecules, in absence or in presence of F10. They measured the absorption coefficient for three different samples in liquid phase ($\sim\mu$m thickness): H9 HA, H9 HA with F10 (specific antibody) and H9 HA with irmAb (non specific antibody). Figure 2 shows the absorption coefficient vs ratio of binding sites (that takes into account both protein and antibody concentrations) for the three samples [55]. The absorption coefficients for H9 HA and H9 HA-irmAb show a non monotonous behavior indicating a hydration shell formation. The H9 HA-F10 sample, instead, present a monotonous behavior with no evidence of hydration. This trend highlights the consequence of binding sites of the antibody-antigen reaction on the protein configuration. Thus, using the capabilities of THz spectroscopy for probing antibody-antigen binding, the optical properties provide a sensitive approach to monitor the H9 HA-F10 interaction. The concentration detection limit was 15 μg ml^{-1}, compared to 113 μg ml^{-1}, determined by ELISA assay. THz spectroscopy approach resulted then $\sim$7.5-fold more sensitive compared to standard ELISA [32, 33].

Although a more extensive research should be performed, previous results [50], suggest that a direct virus THz detection is very difficult due to the virus low THz absorption coefficient and the absence of specific THz spectral features. On the contrary, indirect methods can be successfully used to investigate antibody-antigen reactions, as reported by Sun and coauthors [55]. Those results also suggest that efficient devices, for example based on graphene [56] or on micro-fluidic chips [57], and novel materials like meta-

and nano-materials should be developed for increasing sensitivity and chemical specificity of THz radiation in this vibrating research field [56]. As reported by Zhou *et al* [56], graphene exhibits very fascinating electrical and optical properties, with the possibility to increase the sensitivity by graphene plasmonics and also it can be efficiently used for detecting biomolecules. Moreover, micro-fluidic chips [57] are of great interest because they allow to use extremely small liquid volumes, limiting the strong water absorption in the THz range. In addition, molecules can be trapped within a very small region in the microfluidic channels, providing very concentrated measurements.

3. Meta- and nano-materials

Metamaterial based chips are artificially structured devices with a wide variety of metallic structures with sub-wavelength [56, 58–62]. They gained popularity because of their operational simplicity, compactness and point-of-care suitability. They show attractive electromagnetic properties, mostly related to the excitations of surface plasmon polaritons (SPPs) [63–65], including the capability to extremely localize and enhance the electric field associated to the incoming radiation [50]. Sample deposition on metamaterial devices produces a variation in their dielectric properties, changing the SPPs propagation and interaction with the electromagnetic radiation [64]. In particular, THz metamaterials chips may have single- or multi-resonance frequencies f_0^n exploiting their frequency shift Δf due to sample deposition. f_0^n strictly depend on the unit cell geometry and on the substrate refractive index [25, 50, 66–68]. The local dielectric changes caused by virus, proteins, nucleic acids and other biological samples can be efficiently detected by using metamaterials. Indeed, as very thin water layers ($\sim$20 μm) are needed, the limitations imposed by the strong water absorption coefficient in the THz range can be easily overcome [69].

Sample discrimination takes into account (1) the resonance frequency shift Δf and (2) the relative variation of optical response (OR) (typically transmittance, absorbance or reflectance) at the resonance frequencies f_0^n. This variation is generically labeled with $\Delta OR = OR_{SUB} - OR_{SAMP}$, where OR_{SUB} and OR_{SAMP} are the substrate and sample optical responses at the initial and final (after the interaction) resonance frequencies, respectively [25, 50].

The sensitivity of these metamaterial devices is commonly defined through:

(a) in refractive index n unit (RIU) [70]

$$S_1 = \frac{\Delta f}{\Delta n}\left[\frac{GHz}{RIU}\right], \tag{1}$$

(b) in virus surface number density unit $\left(N_{av} = \frac{N_{virus}}{AREA}\right)$ [25, 69]

$$S_2 = \frac{\Delta f}{N_{av}}\left[\frac{GHz \cdot \mu m^2}{particle}\right]. \tag{2}$$

Being the sensitivity in equations (1) and (2) proportional to Δf, an appropriate design of the metamaterial unit cell area is crucial to enhance the detection capability, shifting the resonant peaks to the desired modes [71]. Many shapes and substrate refractive indexes have been proposed to efficiently fabricate these devices. For instance, periodically repeated split-rings resonators [25], rectangular slots [50], planar Jerusalem crosses [64], H-shaped graphene resonators [70] have been proposed. In figure 3, a schematic picture of the metamaterial unit cell used in [25, 50, 64, 70] is reported.

Recently, nanostructures such as nanogaps have been embedded in metamaterials by nanolithography. Researchers demonstrated that the reduction of the substrate refractive index and the gap width leads to an improvement of sensitivity [69, 72]. However, the sensor specification can be only obtained with functionalization: the biomolecules and/or other biological components are anchored on the meta- and nano-materials. For example, functionalized metamaterials [73–75] with alkanethiol molecules of well-ordered covalent bonded monolayers, or surface chemical modification using silane and silanol chemistries [76–78], CO_x-H modification, anchoring and/or decorating with antigens [79], have been proposed. Moreover, gold nanoparticles (GNPs) have been used, in the THz spectral range, also in combination with metamaterial chips [56, 80]. Ahmadivand *et al* [80] exploited GNPs to effectively detect ZIKV-envelope proteins at low concentration, with a 100-fold enhanced sensitivity.

Hong *et al* [69] proposed their hybrid slot antenna with silver mono-dimensional nanowires. They demonstrated a 2.5-fold sensitivity enhancement, compared to the one without silver nanowires on it.

All these advances in material technology set the scene for extremely promising performance of THz biosensors.

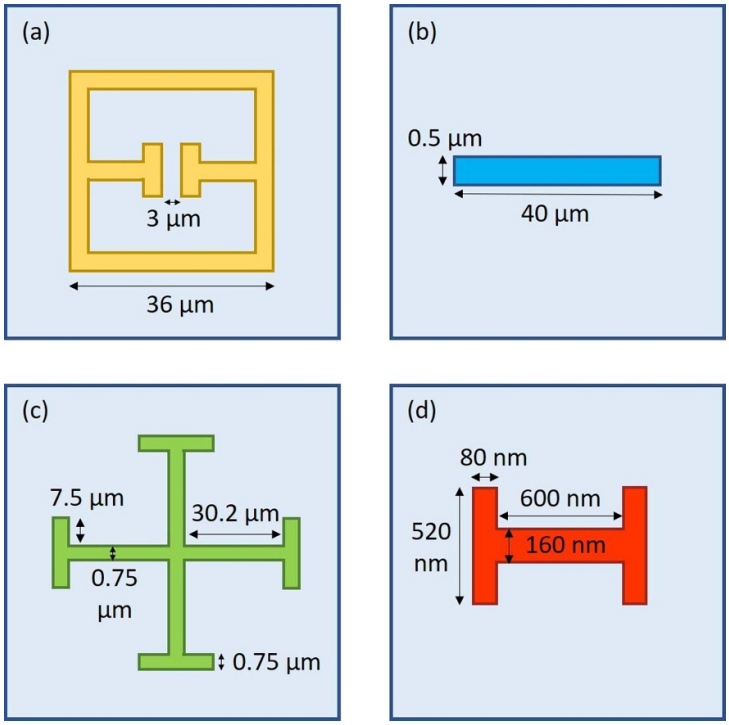

Figure 3. Different geometries of metamaterial unit cell found in literature. (a) Split-rings resonator [25]. (b) Rectangular slot [50]. (c) Planar Jerusalem Cross [64]. (d) H-shaped resonator [70].

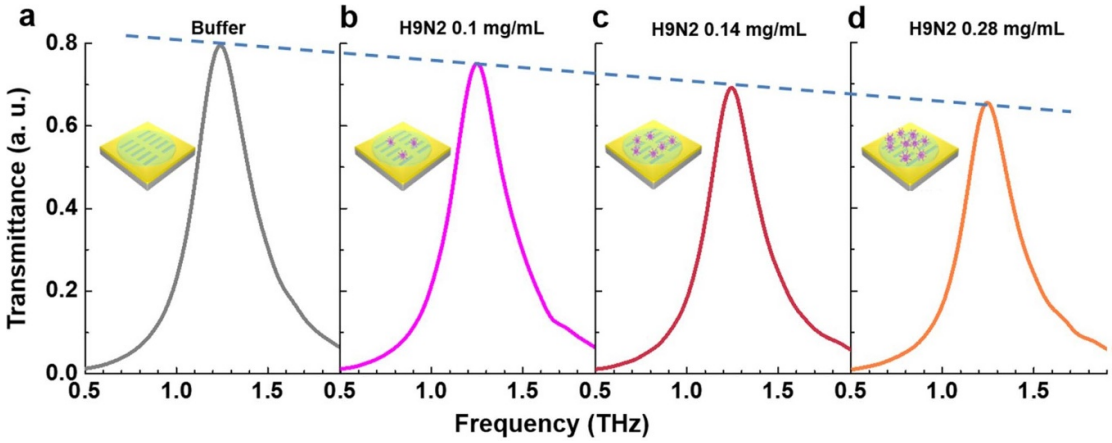

Figure 4. H9N2 Transmittance vs frequency at four sample concentrations. (a) Buffer (0 mg ml^{-1}), (b) 0.10 mg ml^{-1}, (c) 0.14 mg ml^{-1} and (d) 0.28 mg ml^{-1} [50].

Park *et al* [25] fabricated THz split-ring resonators (see figure 3(a)) by e-beam lithography and photolithography. Their metamaterials were prepared both on quartz and on silicon substrate, followed by metal evaporation of Cr (3 nm) and Au (97 nm). They used them for detecting small MS2 and PRD1 viruses (30 and 60 nm, respectively), at low density. They analyzed a 40 μm thick layer for both viruses and obtained information on the viruses dielectric constant (ε_r), lacking in literature.

Successively, the same group performed measurements on both viruses, changing their density and the metamaterial gap widths. They demonstrated that the resonance frequency shift increases with virus surface density until saturation and the sensitivity is higher for smaller metamaterial gap widths (200 nm instead of 3 μm).

Lee *et al* [50] fabricated rectangular nano-antennas (see figure 3(b)) by e-beam lithography, using a silicon wafer patterned with gold (150 nm). They tested their device with periodic rectangular slots for sensing AI virus subtypes: H1N1, H5N2 and H9N2. Authors demonstrated that each virus sample produces a different transmission change and resonance frequency shift, with respect to substrate only. This opens the

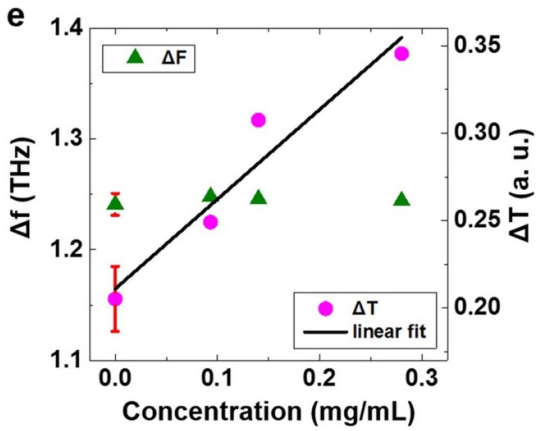

Figure 5. Resonance frequency shift (Δf) and transmittance changes (ΔT) as a function of H9N2 sample concentration [50].

Table 1. Complex refractive indexes used by [50, 64, 70] for modeling H1N1, H5N2, H9N2 virus types.

Virus type	Refractive index (N)	(α,β)
H1N1	$N = n + 1.4ik$	(1,1.4)
H5N2	$N = n + ik$	(1,1)
H9N2	$N = 1.2n + 1.4ik$	(1.2,1.4)

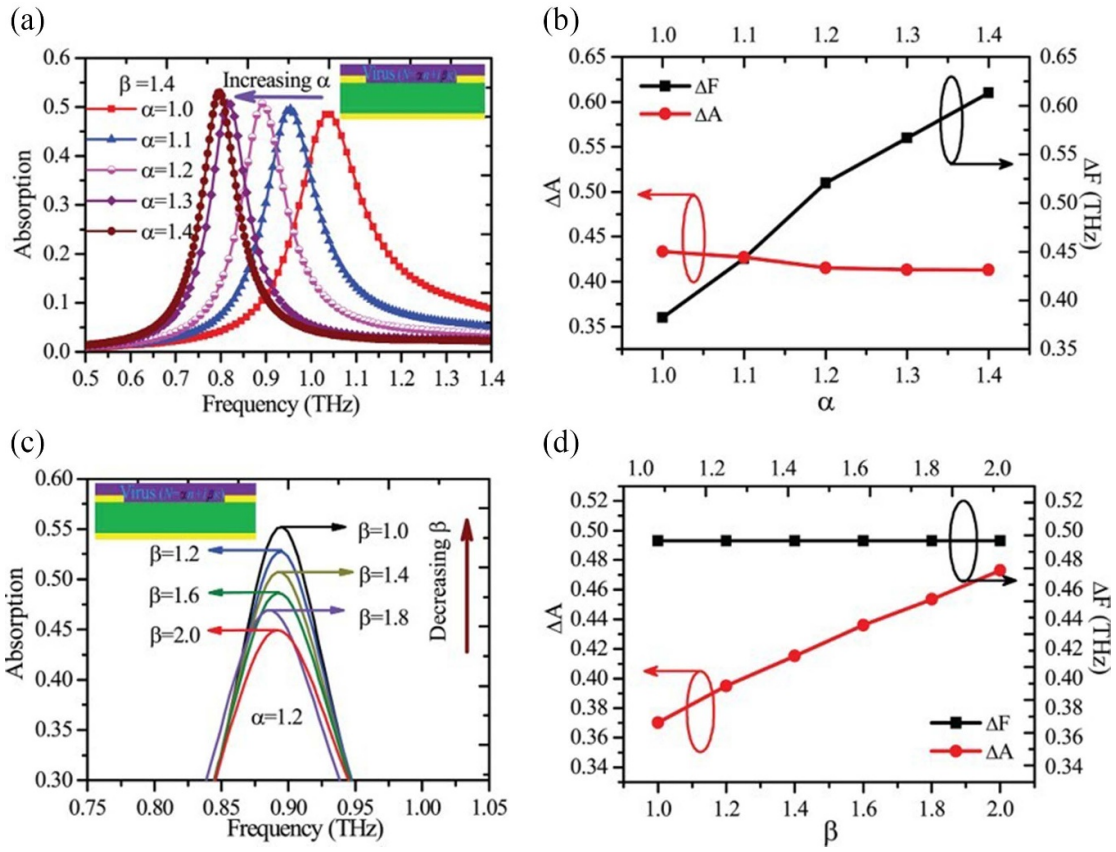

Figure 6. How changes in α and β values yield resonance frequency shifts (ΔF) and absorption differences (ΔA). (a) $1.0 < \alpha < 1.4$, $\beta = 1.4$. (b) ΔF and ΔA as a function of α. ΔF linearly changes with α and ΔA keeps constant. (c) $1.0 < \beta < 2.0$, $\alpha = 1.2$. (d) ΔF and ΔA as a function of β. ΔA linearly changes with α and ΔF keeps constant. Reprinted with permission by [64].

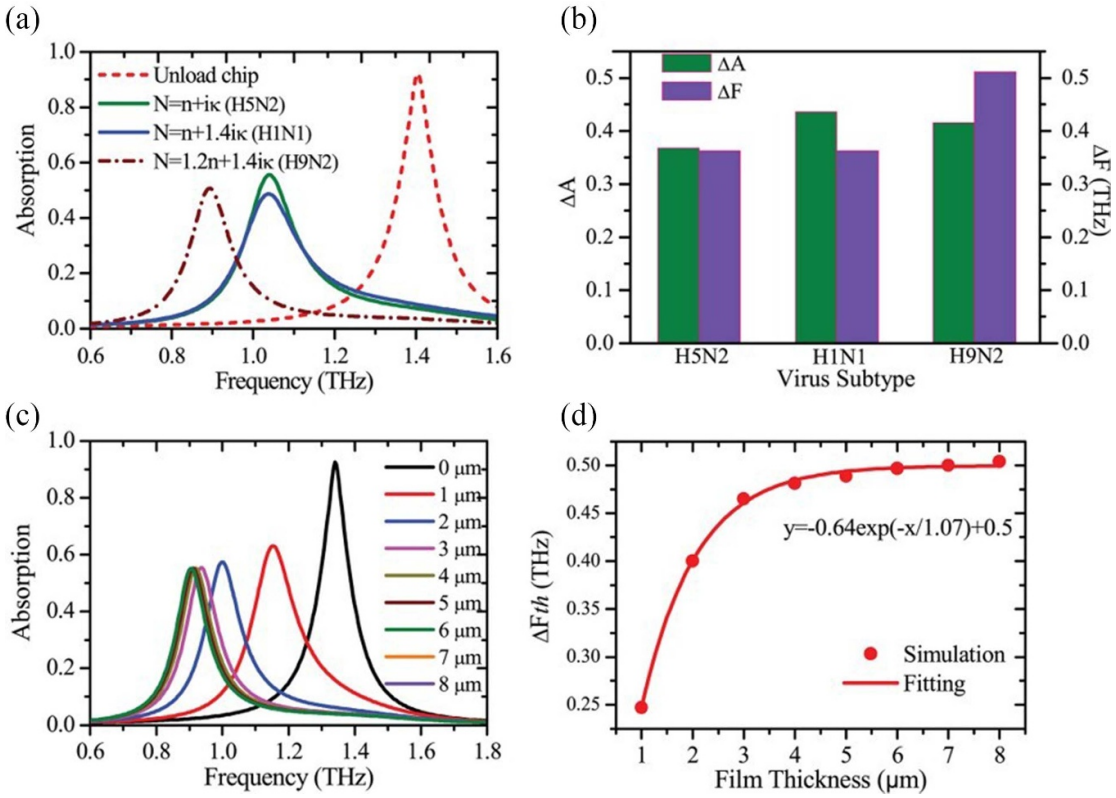

Figure 7. (a) Absorption response of unload chip and three Avian Influenza (AI) virus models (H5N2, H1N1, H9N2) as a function of frequency. (b) Absorption changes (ΔA) and frequency shifts (ΔF) for the three virus modeled subtypes. (c) Resonance frequency shift by increasing the sample thickness. (d) Resonance frequency shift saturation curve as a function of sample thickness. Reprinted with permission by [64].

way to discrimination among different virus types, by looking at ΔOR and Δf. Moreover, Lee *et al* [50] studied H9N2 transmittance, by varying its concentration. Four different concentration values have been chosen (buffer and three virus increasing concentrations). A linear decrease in transmittance value was found, at the resonance frequency, as the concentration increased (see figure 4).

Figure 5 shows resonance frequency (green triangles) and transmittance changes (pink circles) as a function of virus concentration [50]. Note that ΔT linearly changes as a function of sample concentration (see figures 4 and 5), while Δf keeps constant [50].

Finally, Hong *et al* [69] manufactured their hybrid slot antennas on quartz substrate garnishing them with silver nanowires (with 20 nm diameter and 1–5 μm length). They tested their metamaterial on PRD1 virus droplets. Authors observed sensitivity enhancement due to the presence of nanowires. The hybrid chip exhibit a ~2.5 factor enhanced sensitivity S, if compared to the bare chip (S~33 GHz·μm^2/particle instead of ~13 GHz·μm^2/particle). This value can be further improved by performing multi drop-casting and by changing geometrical factors and used substrate materials.

Some groups [50, 64, 70] performed finite-difference time-domain simulations on various metamaterial unit cell chip geometries. Three AI virus samples (H1N1, H5N2 and H9N2) have been modeled as ~μm thick layers, composed by homogeneous dielectric clads. Each virus complex refractive index N has been written as follows:

$$N = \alpha n + i\beta k, \tag{3}$$

where α and β are frequency independent parameters. (α, β) pairs are distinctive of different viruses and their concentrations. n and k are the real and imaginary part of $\tilde{n} = \sqrt{\tilde{\epsilon}}$, respectively [50, 64]. In particular, viruses have been described using the parameters listed in table 1.

Lee and collaborators [50] found a great accordance between experimental and simulated data on the three virus types. H1N1 and H5N2 share the same Δf, while H1N1 and H9N2 the same ΔT. This finding is directly related to the (α, β) values. α is responsible of resonance frequency shift, while β of transmittance changes. Therefore, as H1N1 and H5N2 share the same α, they will experience the same Δf. The same applies for β and ΔT.

Cheng and coauthors [64], with their Planar Jerusalem Cross structures (figure 3(c)) confirmed Lee *et al* [50] results by varying (α, β) pairs and looking at resonance frequency shifts and absorption changes. They modeled their 5 μm thick samples and the results are reported in figure 6. In figure 6(a) they kept $\beta = 1.4$ and varied α between 1.0 and 1.4. They demonstrated that, as α increases, the resonance frequency linearly decreases, therefore the resonance frequency shift ΔF linearly increases, while absorption (Δ A) values remain almost constant (see figure 6(b)). The opposite trend has been verified for β, as shown in figures 6(c) and (d).

In figure 7(a) the simulated absorption response for three AI virus types is reported. The viruses are modeled by different (α, β) values, as reported in table 1. The histogram in figure 7(b) shows absorption differences and resonance frequency shifts. Thereby, all these virus models confirm the efficient discrimination by looking at Δ F and Δ A. Finally, more interestingly, Cheng *et al* [64] simulated how the increasing sample thickness (from 1 to 8 μm) affects the resonance frequency shift. They found a saturation effect (see figures 7(c) and (d)), verifying the saturation-thickness behavior exploited by Park *et al* [25] in their measurements.

4. Conclusion and perspectives

The demand for large-scale tools to detect viruses in quick and effective modalities has grown and is continuously increasing, in the light of pandemic events of the last two decades. Although many molecular techniques (RT-PCR, bDNA, RT-LAMP etc) are currently available and successfully used, they are still complex and difficult to apply on a large-scale. In this framework, THz technology has some characteristics that make it suitable for biosensing applications, such as pathogens, complementing or enhancing conventional solutions. This short review emphasizes the possibility to sense and identify viruses with THz radiation. In the first part, we focused on traditional THz sensing, such as THz-TDS, which does not reach a good sensitivity to monitor and/or discriminate the virus presence, unless indirect investigations are preferred. In the second part of this review, we dealt with the effective THz virus sensing using meta- and nano-sensors. Both experiments and simulations were reported to demonstrate the great potentialities of virus detection with metamaterial chips. Different unit cells geometries were studied in order to push over the detection limit. Meta- and nano-materials, operating in the THz regime, are an emerging alternative with a great potential for high-speed and on-site virus detection. The recent technological improvements in manufacturing techniques promise to extend the performances of meta- and nano-sensors, achieving sensitivity values much higher than traditional/conventional tools. Consequently, this research topic, although started merely few years ago, has grown and reached a discrete maturity, and it is destined to hold a relevant position in the future.

Data availability statement

No new data were created or analyzed in this study.

Funding

We thank for funding the Italian Ministry of Foreign Affairs and International Cooperation (MAECI) in the framework of the Great Relevance Bilateral Project PGR01020 between Italy and China. We also thank BRIC-INAIL project ID12.

ORCID iDs

Marta Di Fabrizio https://orcid.org/0000-0003-3812-5995
Stefano Lupi https://orcid.org/0000-0001-7002-337X
Annalisa D'Arco https://orcid.org/0000-0001-7990-5117

References

[1] Harrap K A 1972 The structure of nuclear polyhedrosis viruses: II. The virus particle *Virology* **50** 124–32
[2] Li-Fang H, Alling D, Popkin T, Shapiro M, Alter H J and Purcell R H 1987 Determining the size of non-a, non-b hepatitis virus by filtration *J. Infectious Dis.* **156** 636–40
[3] Rossmann M G 2013 Structure of viruses: a short history *Q. Rev. Biophys.* **46** 133
[4] Yu I T S, Yuguo Li, Wong T W, Tam W, Chan A T, Lee J H W, Leung D Y C and Tommy H 2004 Evidence of airborne transmission of the severe acute respiratory syndrome virus *New Engl. J. Med.* **350** 1731–9
[5] Morawska L and Cao J 2020 Airborne transmission of SARS-CoV-2: the world should face the reality *Environ. Int.* **139** 105730

[6] Bosch A *et al* 2011 Analytical methods for virus detection in water and food *Food Anal. Methods* **4** 4–12
[7] Miranda R C and Schaffner D W 2019 Virus risk in the food supply chain *Curr. Opin. Food Sci.* **30** 43–8
[8] Shattock R J and Moore J P 2003 Inhibiting sexual transmission of HIV-1 infection *Nat. Rev. Microbiol.* **1** 25–34
[9] Musso D, Roche C, Robin E, Nhan T, Teissier A and Van-Mai C-L 2015 Potential sexual transmission of Zika virus *Emerg. Infectious Dis.* **21** 359
[10] D'Ortenzio E *et al* 2016 Evidence of sexual transmission of Zika virus *New Engl. J. Med.* **374** 2195–8
[11] Costa Secundino N F *et al* 2017 Zika virus transmission to mouse ear by mosquito bite: a laboratory model that replicates the natural transmission process *Parasites Vectors* **10** 346
[12] Jartti T, Söderlund-Venermo M, Hedman K, Ruuskanen O and Mäkelä M J 2013 New molecular virus detection methods and their clinical value in lower respiratory tract infections in children *Paediatric Resp. Rev.* **14** 38–45
[13] Notomi T, Mori Y, Tomita N and Kanda H 2015 Loop-mediated isothermal amplification (LAMP): principle, features and future prospects *J. Microbiol.* **53** 1–5
[14] Thompson D and Lei Y 2020 Mini review: recent progress in RT-LAMP enabled COVID-19 detection *Sens. Actuators Rep.* **2** 100017
[15] Kellner M J, Koob J G, Gootenberg J S, Abudayyeh O O and Zhang F 2019 SHERLOCK: nucleic acid detection with CRISPR nucleases *Nat. Protocols* **14** 2986–3012
[16] Patchsung M *et al* 2020 Clinical validation of a Cas13-based assay for the detection of SARS-CoV-2 RNA *Nat. Biomed. Eng.* **4** 1–10
[17] Zaytseva N V, Montagna R A and Baeumner A J 2005 Microfluidic biosensor for the serotype-specific detection of dengue virus RNA *Anal. Chem.* **77** 7520–7
[18] Liu W-T, Zhu L, Qin Q-W, Zhang Q, Feng H and Ang S 2005 Microfluidic device as a new platform for immunofluorescent detection of viruses *Lab on a Chip* **5** 1327–30
[19] Yu-Dong M, Chen Y-S and Lee G-B 2019 An integrated self-driven microfluidic device for rapid detection of the influenza A (H1N1) virus by reverse transcription loop-mediated isothermal amplification *Sens. Actuators* B **296** 126647
[20] Berkenbrock J A, Grecco-Machado R and Achenbach S 2020 Microfluidic devices for the detection of viruses: aspects of emergency fabrication during the COVID-19 pandemic and other outbreaks *Proc. R. Soc.* A **476** 20200398
[21] Udugama B *et al* 2020 Diagnosing COVID-19: the disease and tools for detection *ACS Nano* **14** 3822–35
[22] Long Q-X *et al* 2020 Antibody responses to SARS-CoV-2 in patients with COVID-19 *Nat. Med.* **26** 1–4
[23] Tsongalis G J 2006 Branched DNA technology in molecular diagnostics *Am. J. Clin. Pathol.* **126** 448–53
[24] Ferré F 2012 *Gene Quantification* (Boston: Springer) (https://doi.org/10.1007/978-1-4612-4164-5)
[25] Park S J, Cha S H, Shin G A and Ahn Y H 2017 Sensing viruses using terahertz nano-gap metamaterials *Biomed. Opt. Express* **8** 3551–8
[26] Wald A and Ashley-Morrow R 2002 Serological testing for herpes simplex virus HSV-1 and HSV-2 infection *Clin. Infectious Dis.* **35** S173–82
[27] Breuer J, Scott Schmid D and Gershon A A 2008 Use and limitations of varicella-zoster virus-specific serological testing to evaluate breakthrough disease in vaccinees and to screen for susceptibility to varicella *J. Infectious Dis.* **197** S147–51
[28] Lee W T *et al* 2018 Development of Zika virus serological testing strategies in New York State *J. Clin. Microbiol.* **56** JCM.01591-17
[29] Bastos M L *et al* 2020 Diagnostic accuracy of serological tests for Covid-19: systematic review and meta-analysis *BMJ* **370** m2516
[30] La Marca A, Capuzzo M, Paglia T, Roli L, Trenti T and Nelson S M 2020 Testing for SARS-CoV-2 (COVID-19): a systematic review and clinical guide to molecular and serological in-vitro diagnostic assays *Reprod. Biomed. Online* **41** 483–99
[31] Lin D *et al* 2020 Evaluations of the serological test in the diagnosis of 2019 novel coronavirus (SARS-CoV-2) infections during the COVID-19 outbreak *Eur. J. Clin. Microbiol. Infectious Dis.* **39** 1–7
[32] Reen D J 1994 Enzyme-linked immunosorbent assay (ELISA) *Basic Protein and Peptide Protocols* (Berlin: Springer) pp 461–6
[33] Gan S D and Patel K R 2013 Enzyme immunoassay and enzyme-linked immunosorbent assay *J. Invest. Dermatol.* **133** e12
[34] Ghann W and Uddin J 2017 Terahertz (THz) spectroscopy: a cutting edge technology *Terahertz Spectroscopy—A Cutting Edge Technology*
[35] Zaytsev K I *et al* 2019 The progress and perspectives of terahertz technology for diagnosis of neoplasms: a review *J. Opt.* **22** 013001
[36] Okada K *et al* 2019 Scanning laser terahertz near-field reflection imaging system *Appl. Phys. Express* **12** 122005
[37] D'Arco A, Di Fabrizio M, Dolci V, Petrarca M and Lupi S 2020 THz pulsed imaging in biomedical applications *Condens. Matter* **5** 25
[38] Di Fabrizio M, D'Arco A, Mou S, Palumbo L, Petrarca M and Lupi S 2021 Performance evaluation of a THz pulsed imaging system: point spread function, broadband THz beam visualization and image reconstruction *Appl. Sci.* **11** 562
[39] Son J-H, Oh S J and Cheon H 2019 Potential clinical applications of terahertz radiation *J. Appl. Phys.* **125** 190901
[40] Hartnagel H L and Sirkeli V P 2019 The use of metal oxide semiconductors for THz spectroscopy of biological applications *Int. Conf. on Nanotechnologies and Biomedical Engineering* (Cham: Springer) pp 213–17
[41] Banerjee A, Vajandar S and Basu T 2020 Prospects in medical applications of terahertz waves *Terahertz Biomedical and Healthcare Technologies* (Amsterdam: Elsevier) pp 225–39
[42] Mittleman D M, Jacobsen R H, Neelamani R, Baraniuk R G and Nuss M C 1998 Gas sensing using terahertz time-domain spectroscopy *Appl. Phys.* B **67** 379–90
[43] Fan S, Jeong K, Wallace V P and Aman Z 2019 Use of terahertz waves to monitor moisture content in high-pressure natural gas pipelines *Energy Fuels* **33** 8026–31
[44] D'Arco A, Tomarchio L, Dolci V, Di Pietro P, Perucchi A, Mou S, Petrarca M and Lupi S 2020 Broadband anisotropic optical properties of the terahertz generator HMQ-TMS organic crystal *Condens. Matter* **5** 47
[45] D'Arco A *et al* 2020 Fabrication and spectroscopic characterization of graphene transparent electrodes on flexible cyclo-olefin substrates for terahertz electro-optic applications *Nanotechnology* **31** 364006
[46] Islam Md S, Sultana J, Ahmed K, Islam M R, Dinovitser A, Wai-Him Ng B and Abbott D 2017 A novel approach for spectroscopic chemical identification using photonic crystal fiber in the terahertz regime *IEEE Sens. J.* **18** 575–82
[47] D'Arco A, Di Fabrizio M, Dolci V, Marcelli A, Petrarca M, Della Ventura G and Lupi S 2020 Characterization of volatile organic compounds (VOCs) in their liquid-phase by terahertz time-domain spectroscopy *Biomed. Opt. Express* **11** 1–7
[48] Zhang Xi-C and Jingzhou X 2010 *Introduction to THz Wave Photonics* vol 29 (Berlin: Springer) (https://doi.org/10.1007/978-1-4419-0978-7)
[49] Manti L and D'Arco A 2010 Cooperative biological effects between ionizing radiation and other physical and chemical agents *Mutation Rese./Rev. Mutation Res.* **704** 115–22
[50] Lee D-K *et al* 2017 Nano metamaterials for ultrasensitive terahertz biosensing *Sci. Rep.* **7** 1–6
[51] Lee Y-S 2009 *Principles of Terahertz Science and Technology* vol 170 (Boston: Springer) (https://doi.org/10.1007/978-0-387-09540-0)

[52] Yang X, Zhao X, Yang K, Liu Y, Liu Y, Fu W and Luo Y 2016 Biomedical applications of terahertz spectroscopy and imaging *Trends Biotechnol.* **34** 810–24
[53] Abbe E 1873 Beiträge zur theorie des mikroskops und der mikroskopischen wahrnehmung *Archiv für Mikroskopische Anatomie* **9** 413–68
[54] Ajito K and Ueno Y 2011 THz chemical imaging for biological applications *IEEE Trans. Terahertz Sci. Technol.* **1** 293–300
[55] Sun Y, Zhong J, Zhang C, Zuo J and Emma P-M 2015 Label-free detection and characterization of the binding of hemagglutinin protein and broadly neutralizing monoclonal antibodies using terahertz spectroscopy *J. Biomed. Opt.* **20** 037006
[56] Zhou R, Wang C, Wendao X and Xie L 2019 Biological applications of terahertz technology based on nanomaterials and nanostructures *Nanoscale* **11** 3445–57
[57] Tang Q, Liang M, Yi L, Wong P K, Wilmink G J, Zhang D D and Xin H 2016 Microfluidic devices for terahertz spectroscopy of live cells toward lab-on-a-chip applications *Sensors* **16** 476
[58] Chen X and Fan W 2017 Ultrasensitive terahertz metamaterial sensor based on spoof surface plasmon *Sci. Rep.* **7** 1–8
[59] Wendao X, Xie L and Ying Y 2017 Mechanisms and applications of terahertz metamaterial sensing: a review *Nanoscale* **9** 13864–78
[60] Samy Saadeldin A, Hameed M F O, Elkaramany E M A and Obayya S S A 2019 Highly sensitive terahertz metamaterial sensor *IEEE Sens. J.* **19** 7993–9
[61] Ahmadivand A, Gerislioglu B, Ahuja R and Mishra Y K 2020 Terahertz plasmonics: the rise of toroidal metadevices towards immunobiosensings *Mater. Today* **32** 108–30
[62] Díaz M B and Jáuregui López I 2020 Terahertz sensing based on metasurfaces *Adv. Opt. Mater.* **8** 1900721
[63] Zhang Y and Han Z 2015 Spoof surface plasmon based planar antennas for the realization of terahertz hotspots *Sci. Rep.* **5** 18606
[64] Cheng D, Xia H, Huang X, Zhang B, Liu G, Shu G, Fang C, Wang J and Luo Y 2018 Terahertz biosensing metamaterial absorber for virus detection based on spoof surface plasmon polaritons *Int. J. RF Micro. Computer-Aided Eng.* **28** e21448
[65] Tang W X, Zhang H C, Ma H F, Jiang W X and Cui T J 2019 Concept, theory, design and applications of spoof surface plasmon polaritons at microwave frequencies *Adv. Opt. Mater.* **7** 1800421
[66] Limaj O, Nucara A, Lupi S, Ortolani M, Di Gaspare A, Palange E and Carelli P 2011 Scaling the spectral response of metamaterial dipolar filters in the terahertz *Opt. Commun.* **284** 1690–3
[67] D'Apuzzo F *et al* 2015 Resonating terahertz response of periodic arrays of subwavelength apertures *Plasmonics* **10** 45–50
[68] D'Apuzzo F *et al* 2017 Terahertz and mid-infrared plasmons in three-dimensional nanoporous graphene *Nat. Commun.* **8** 14885
[69] Hong J T, Jun S W, Cha S H, Park J Y, Lee S, Shin G A and Ahn Y H 2018 Enhanced sensitivity in THz plasmonic sensors with silver nanowires *Sci. Rep.* **8** 1–8
[70] Keshavarz A and Vafapour Z 2019 Sensing Avian influenza viruses using terahertz metamaterial reflector *IEEE Sens. J.* **19** 5161–6
[71] Xia X, Sun Y, Yang H, Feng H, Wang Li and Gu C 2008 The influences of substrate and metal properties on the magnetic response of metamaterials at terahertz region *J. Appl. Phys.* **104** 033505
[72] Chen X *et al* 2013 Atomic layer lithography of wafer-scale nanogap arrays for extreme confinement of electromagnetic waves *Nat. Commun.* **4** 1–7
[73] Tantakitti F, Burk-Rafel J, Cheng F, Egnatchik R, Owen T, Hoffman M, Weiss D N and Ratner D M 2012 Nanoscale clustering of carbohydrate thiols in mixed self-assembled monolayers on gold *Langmuir* **28** 6950–9
[74] Xiaojun W, Quan B, Pan X, Xinlong X, Xinchao L, Changzhi G and Wang Li 2013 Alkanethiol-functionalized terahertz metamaterial as label-free, highly-sensitive and specific biosensor *Biosens. Bioelectron.* **42** 626–31
[75] Lee H-J, Lee J-H and Jung H-I 2011 A symmetric metamaterial element-based RF biosensor for rapid and label-free detection *Appl. Phys. Lett.* **99** 163703
[76] Terracciano M, Rea I, Politi J and De Stefano L 2013 Optical characterization of aminosilane-modified silicon dioxide surface for biosensing *J. Eur. Opt. Soc.-Rap. Publications* **8** 13075
[77] De Stefano L, Oliviero G, Amato J, Borbone N, Piccialli G, Mayol L, Rendina I, Terracciano M and Rea I 2013 Aminosilane functionalizations of mesoporous oxidized silicon for oligonucleotide synthesis and detection *J. R. Soc. Interface* **10** 20130160
[78] Terracciano M, Galstyan V, Rea I, Casalino M, De Stefano L and Sbervegleri G 2017 Chemical modification of TiO2 nanotube arrays for label-free optical biosensing applications *Appl. Surf. Sci.* **419** 235–40
[79] Bhardwaj S K, Bhardwaj N, Kumar V, Bhatt D, Azzouz A, Bhaumik J, Kim K-H and Deep A 2021 Recent progress in nanomaterial-based sensing of airborne viral and bacterial pathogens *Environ. Int.* **146** 106183
[80] Ahmadivand A, Gerislioglu B, Tomitaka A, Manickam P, Kaushik A, Bhansali S, Nair M and Pala N 2018 Extreme sensitive metasensor for targeted biomarkers identification using colloidal nanoparticles-integrated plasmonic unit cells *Biomed. Optics Express* **9** 373–86